

# Coarsening behaviour of $\gamma''$ - and $\gamma'$ -particles in Inconel alloy 718

Ya-fang Han, P. Deb, and M. C. Chaturvedi

The coarsening behaviour of disc-shaped, ordered bct  $\gamma''$ -phase, and spherical ordered fcc  $\gamma'$ -phase particles in Inconel alloy 718\* has been studied. In the 973–1023 K temperature range, used in the present investigation, both the phases are present and precipitate coherently in the fcc matrix. The coarsening kinetics of both the phases follow the time-law predictions of the Lifshitz–Wagner theory of diffusion-controlled growth at all the aging temperatures. The actual particle size distribution, however, differs significantly from the theoretically predicted distribution which could be attributed to the effect of ‘encounter’ between the growing particles and could also be due to a large lattice misfit between the precipitate and the matrix.

MS/0764

© 1982 The Metals Society. Manuscript received 3 August 1981; in final form 7 December 1981. Ya-fang Han, P. Deb, and Professor M. C. Chaturvedi are in the Department of Mechanical Engineering, The University of Manitoba, Winnipeg, Canada.

The growth of precipitate particles in precipitation-hardened alloys is of major significance as it can control the long-term mechanical properties of these alloys. The growth of  $\gamma'$ -precipitate particles, which have an ordered fcc structure and precipitate coherently in many Ni-containing fcc alloys, has been accounted for by the theory of diffusion-controlled growth based on the growth theory of Lifshitz and Slyozov<sup>1</sup> and Wagner<sup>2</sup> (LSW theory). The salient features of the LSW theory are as follows: (i) the driving force for the coarsening process is the change in free energy due to a decrease in the particle/matrix interfacial area; (ii) the average particle size is proportional to the cube root of the aging time; (iii) the activation energy for the coarsening process is equal to that for the diffusion of solute atoms in the matrix; and (iv) the particle size distribution at any time  $t$  is independent of the distribution at the onset of the coarsening process and the maximum particle size is 1.5 times the average particle size. In many Ni-containing alloys, the main strengthening phase is observed to be  $\gamma'$  which has an ordered fcc structure and precipitates coherently. The growth of  $\gamma'$ -particles in a number of alloy systems, encompassing a range of volume fractions, coherency strains, and spherical as well as cuboidal shape, follows the  $d \propto t^{1/3}$  law.<sup>3–7</sup> Another commonly observed strengthening phase in many nickel alloys is  $\gamma''$  which has a

bct structure and precipitates coherently with a disc shape. The growth of this phase not only follows the  $t^{1/3}$  law<sup>8–10</sup> but also the  $t^{1/2}$  law.<sup>11</sup> In an Ni–Ta–Fe alloy system, however, the diameter of  $\gamma''$  precipitates grows linearly with time and its thickness follows the  $t^{1/2}$  law.<sup>12</sup> In this system when 1%Al is added,  $\gamma'$ -precipitate also forms which obeys the  $t^{1/3}$  law. In a commercial superalloy, Inconel alloy 718, the major precipitating phases are observed to be ordered bct  $\gamma''$ -phase and ordered fcc  $\gamma'$ -phase.<sup>13</sup> This paper describes the coarsening behaviour of  $\gamma''$ - and  $\gamma'$ -precipitate particles in Inconel 718 over a range of aging temperatures and time.

## EXPERIMENTAL TECHNIQUES

5.0 mm thick sheet of Inconel 718 (the chemical composition of which is listed in Table 1) was provided by the International Nickel Co., Canada. This sheet was cold rolled to 0.2 mm thick strips, with intermediate anneals at 1473 K, which were used for the various aging treatments. All the heat treatments were carried out with specimens sealed in Vycor capsules partially filled with argon. On water quenching, the capsules were always broken under water. Thin films for electron microscopy were prepared by electropolishing 3 mm discs of heat-treated strips in a jet electropolishing unit using 15% perchloric acid, 85% methanol bath at 223–233 K. It has been observed<sup>13</sup> that in Inconel 718 the  $\gamma''$ -phase grows coherently into discs on {100} planes of the fcc matrix with the  $c$  axis of  $\gamma''$ -phase being perpendicular to the discs. The  $\gamma'$ -phase also forms coherently on the {100} matrix planes. Due to the presence of large coherency strains around  $\gamma''$ - and  $\gamma'$ -precipitates individual particles could be observed only in the dark-field micrographs taken with their superlattice reflections. Also, to determine the true sizes of  $\gamma''$ - and  $\gamma'$ -particles, their dimensions were measured in only {100} thin-foil orientation. About 200–300 individual  $\gamma''$ - and  $\gamma'$ -particles were measured after each aging treatment to establish their growth rate and size distribution. The number of particles/unit volume  $N_v$  was calculated from the number of particles/unit area  $N_a$  by the expression  $N_v = N_a/(\bar{d} + t)$ , as suggested by Cahn and Nutting,<sup>14</sup> where  $t$  is the foil thickness and  $\bar{d}$  is the average particle size. The combined volume fraction of ( $\gamma' + \gamma''$ )-phase was determined by electrochemical extraction of the precipitate particles in 1% ammonium sulphate and 1% citric acid in distilled water. By electron microscopy, the ratio of the volume fraction of  $\gamma''$  to  $\gamma'$  was found to be between 2.5 and 4.0 which is in good agreement with the previously reported value of 3.0.<sup>13</sup>

## RESULTS

The specimens were given a final solution treatment at 1473 K for 1 h and quenched in water. They were then aged at 973, 998, and 1023 K for various lengths of time. The

\* Inconel is a trade mark of Huntington Alloys Incorporated.

**Table 1** Chemical composition of Inconel alloy 718, wt-%

C	Fe	Ni	Cr	Al	Ti	Mo	Cb+Ta	Mn	S	Si	Cu
0.03	19.24	52.37	18.24	0.52	0.97	3.07	4.94	0.19	0.007	0.30	0.04

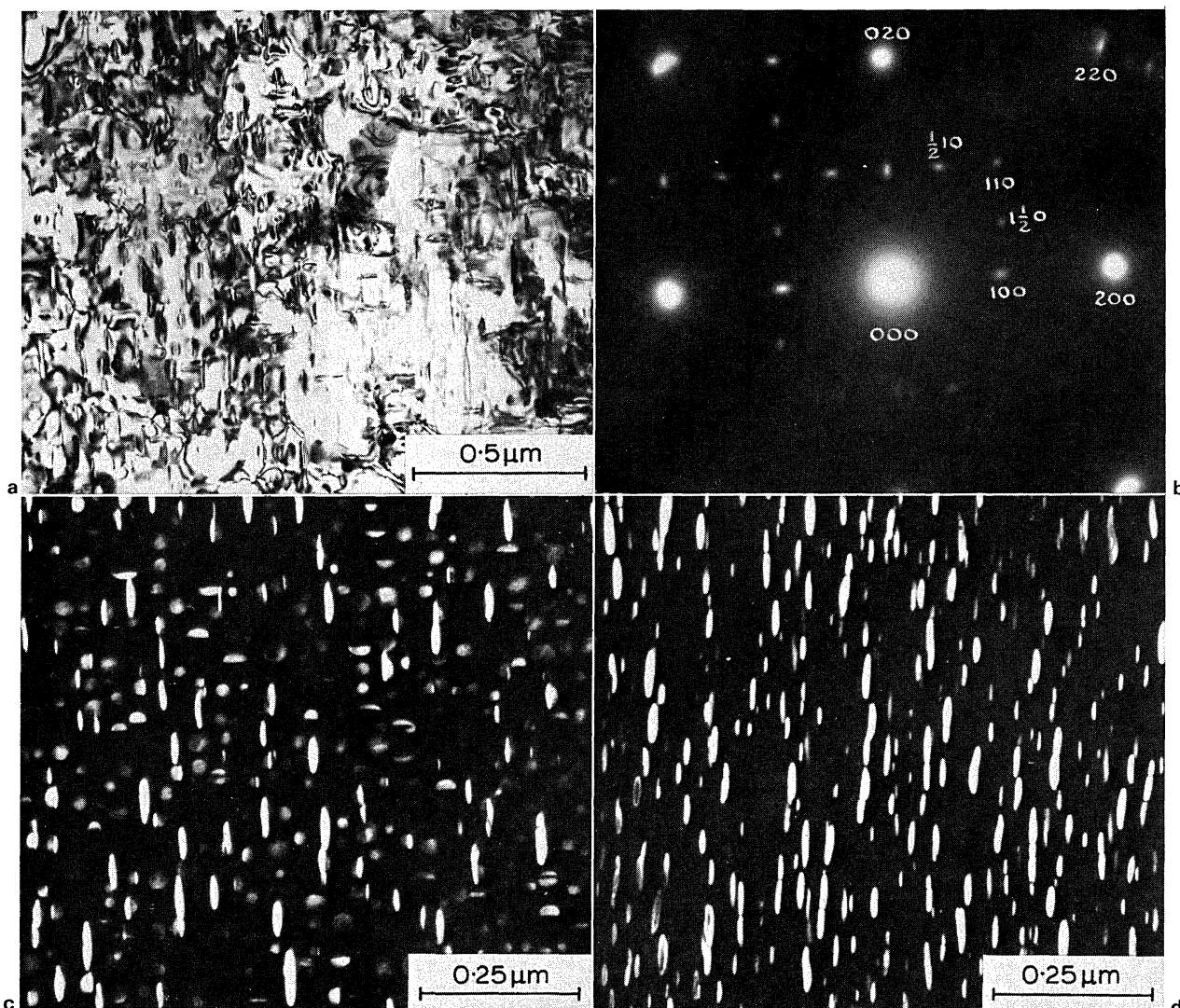
precipitation behaviour of this alloy was similar to that reported by Paulonis *et al.*<sup>13</sup> A typical aged structure is shown in Fig. 1a and b which shows the bright-field microstructure and selected-area diffraction pattern (SADP), respectively, of a specimen aged for 200 h at 998 K. The secondary diffraction spots in SADP are due to the presence of ordered  $\gamma'$ - and  $\gamma''$ -precipitate particles. The (100), (010), and (110) reflections in SADP are both due to the  $\gamma'$ - and  $\gamma''$ -phases whereas, (1/2 10)-type reflections are only due to the  $\gamma''$ -phase. This is evidenced by the dark-field structure shown in Fig. 1c which is taken with (100) reflection. Disc-shape  $\gamma''$ -particles and spherical  $\gamma'$ -particles are visible. However, in Fig. 1d which is taken with (1/2 10) reflection, only disc-shape  $\gamma''$ -particles are observed. A number of dark-field micrographs of areas in (100)

orientation with (1/2 10)  $\gamma''$  and (100)( $\gamma'' + \gamma'$ ) were obtained and their particle sizes were measured. The precipitation reaction at all three aging temperatures was the same except for the total volume fraction of ( $\gamma' + \gamma''$ )-particles which were 17.5, 16.6, and 15.4 at 973, 998, and 1023 K, respectively. The volume fraction at a particular temperature was the same at all the aging times investigated.

### Growth rate

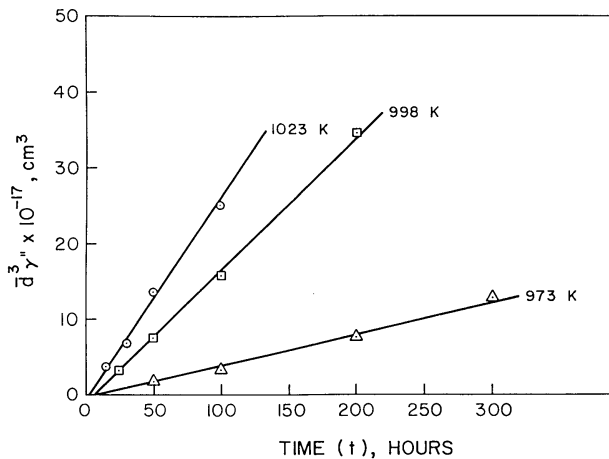
When the growth of a precipitate follows the LSW theory of diffusion-controlled growth, the kinetic equation for the growth of spherical particles can be written as

$$\bar{r}^3 - \bar{r}_0^3 = \frac{8\gamma D C_e V_m^2}{9RT} t = K't \quad (1)$$



a thin-film structure; b selected-area diffraction pattern of thin-film structure with (001) orientation; c, d dark-field micrographs of thin-film structure with c (100)( $\gamma'' + \gamma'$ ) reflection and d (1/2 10) $\gamma''$  reflection

### 1 Specimen aged for 200 h at 998 K

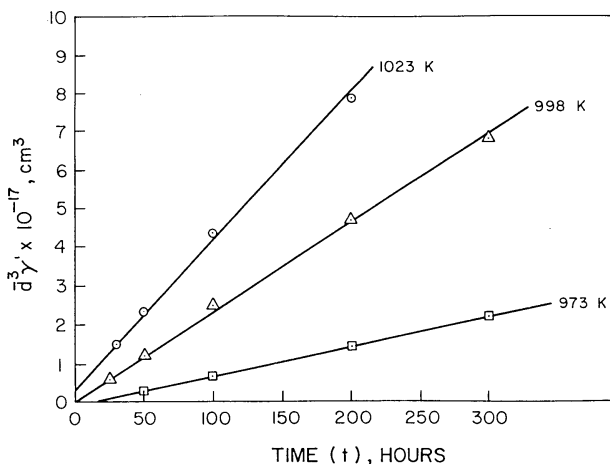


2 Variation in  $\gamma''$ (diameter)<sup>3</sup> with aging time at different aging temperatures

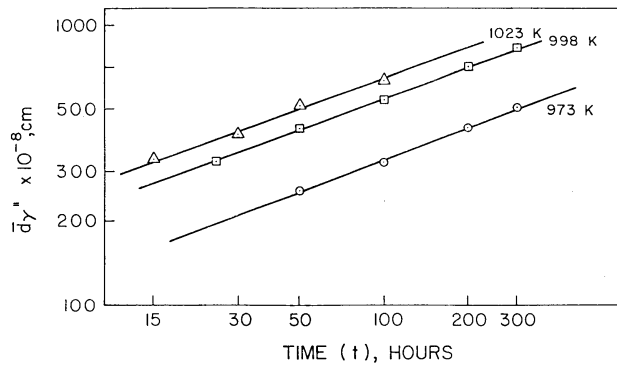
where  $\bar{r}$  is the average radius of the growing particle at time  $t$ ,  $\bar{r}_0$  is the radius at the onset of the coarsening process,  $\gamma$  is the interfacial free energy of the particle/matrix interface,  $D$  is the diffusion coefficient of the solute atoms in the matrix,  $C_e$  is the concentration of solute atoms in equilibrium with a particle of infinite radius,  $R$  is the gas constant,  $T$  is the absolute temperature of coarsening, and  $V_m$  is the molar volume of the precipitate. For disc-shaped particles equation (1) has been modified<sup>15</sup> to

$$\bar{d}^3 - \bar{d}_0^3 = \frac{128\gamma^p q D C_e V_m^2}{9\pi R T} t = K'' t \quad (2)$$

where  $\bar{d}$  is the mean diameter of the disc-shaped particle,  $\gamma^p$  is the interfacial energy of the peripheral interface which is normal to the direction of measurement of  $d$ ,  $q$  is the aspect ratio =  $d/h$ , where  $h$  is the thickness. Therefore, if the disc-shaped  $\gamma''$ -particles grow by volume diffusion a plot of  $\bar{d}^3$  against time  $t$  should be a straight line. Such plots at 973, 998, and 1023 K are shown in Fig. 2. It can be seen that at all three aging temperatures  $\bar{d}^3$  v.  $t$  plots are straight lines suggesting that the  $\gamma''$ -phase in Inconel 718 grows by volume diffusion. Similarly,  $\gamma'$ -phase is also seen to grow by volume diffusion since the  $\bar{d}^3$  v.  $t$  plots for this phase are also straight lines at all three aging temperatures as shown in Fig. 3. The volume diffusion-controlled growth of  $\gamma''$  and  $\gamma'$



3 Variation in  $\gamma'$ (diameter)<sup>3</sup> with aging time at different aging temperatures



4 Log plots of mean particle diameter of  $\gamma''$ -particles v. aging time at different temperatures

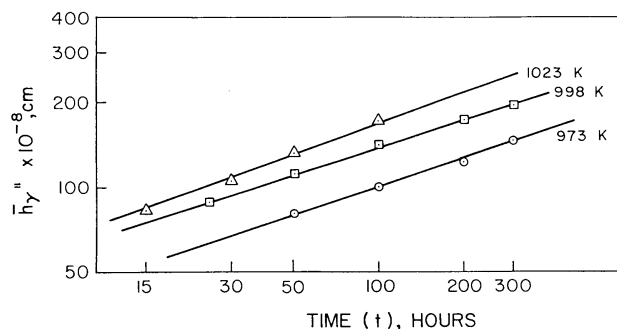
was also established by plotting  $\log(\text{particle size})$  v.  $\log t$  at various aging temperatures. As seen in Figs. 4, 5, and 6, these plots are straight lines. The slope of each of these straight lines, as listed in Table 2, is close to  $1/3$  which also suggests that both  $\gamma''$ - and  $\gamma'$ -phase particles grow by diffusion-controlled growth.

#### Activation energy

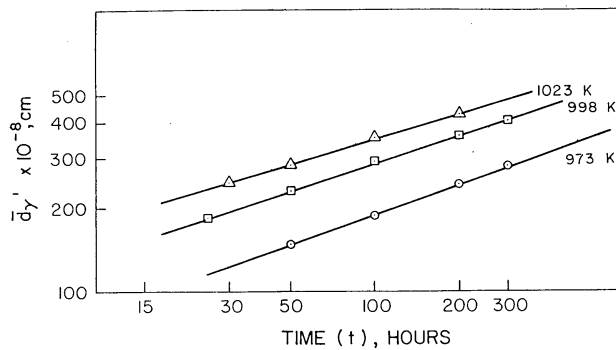
Another postulate of the LSW theory is that the activation energy for the coarsening process should be equal to that for the diffusion of solute atoms in the matrix. Therefore, an attempt was made to determine the activation energy for the coarsening of  $\gamma''$ - and  $\gamma'$ -phases in this alloy. The diffusion coefficient  $D$  in equations (1) and (2), is defined as  $D = D_0 \exp(-Q/RT)$  where  $D_0$  is the frequency factor and  $Q$  is the activation energy. The slope of the straight lines in Fig. 2  $K''$  can be expressed from equation (2) as follows

$$K'' = \frac{128}{9} \frac{\gamma^p C_e V_m^2 D_0}{\pi R} \frac{q}{T} \exp(-Q\gamma''/RT) \quad (3)$$

In this expression,  $K''$ ,  $C_e$ ,  $q$ , and  $T$  are the only temperature-dependent terms. Therefore, if their values at various temperatures are known, the activation energy  $Q\gamma''$  can be determined by the slope of the  $\ln(K''T/qC_e)$  v.  $1/T$  plot. It should be noted that for this complex alloy, unlike in a simple binary system, uncertainties exist regarding the partitioning of various elements in  $\gamma''$ - and  $\gamma'$ -phases, e.g. Nb can substitute for Ti and Al in  $\gamma'$ -phase and Ti and Al can replace part of Nb in  $\gamma''$ -phase. Also the exact ratio of volume fraction of  $\gamma'$ - and  $\gamma''$ -phases is not known. Therefore, it is not possible to determine the activation energy for the coarsening process very accurately. However, it is observed that the total volume fraction of ( $\gamma' + \gamma''$ )



5 Log plots of mean particle thickness of  $\gamma''$ -particles v. aging time at different temperatures



6 Log plots of mean diameter of  $\gamma'$  v. aging time at different temperatures

changes only by about 12% over the temperature range used in the present investigation. Therefore, the value of  $C_e$  may be considered as constant and the activation energy  $Q_{\gamma'}$  can be determined from the slope of the  $\ln(TK''/q)$  v.  $1/T$  plot. The data for the determination of activation energy are given in Table 3, and the  $\ln(TK''/q)$  v.  $1/T$  plot is shown in Fig. 7. It can be seen that this plot is a straight line and the activation energy by the least-squares fit was calculated to be  $298 \pm 41$  KJ mol $^{-1}$ . Similarly, for the  $\gamma'$ -precipitate particles, the slope of the  $\bar{d}^3$  v.  $t$  plots, shown in Fig. 3 can be rewritten from equation (1) as follows

$$K' = \frac{8\gamma C_e V_m D_0}{9R} \frac{1}{T} \exp(-Q_{\gamma'}/RT) \quad (4)$$

Thus, the activation energy for the coarsening of  $\gamma'$ -phase  $Q_{\gamma'}$  can be determined from the slope of the  $\ln(TK')$  v.  $1/T$  plot shown in Fig. 7. The relevant data are given in Table 3 and  $Q_{\gamma'}$  was calculated to be  $271 \pm 49$  KJ mol $^{-1}$ .

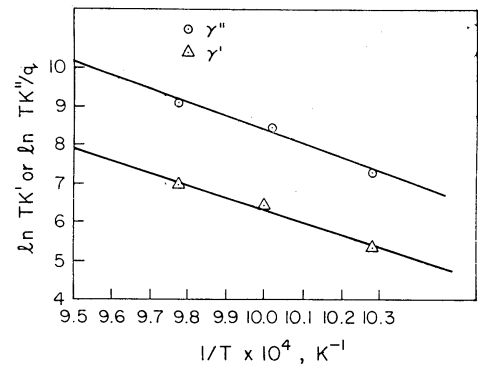
#### Distribution of precipitate particles

The distribution of  $\gamma''$ - and  $\gamma'$ -particle sizes after various aging times was normalized in accordance with the procedure suggested by Ardel and Nicholson.<sup>4</sup> The steady-state distribution of particle sizes  $f(d, t)$  is given by

$$f(d, t) = \frac{N_v}{\bar{d}} \frac{8}{9} \rho^2 h(\rho) \quad (5)$$

Table 2 Slopes of log (particle size) v. log (aging time) plots

Plot	Temperature, K		
	973	998	1023
$\log d\gamma'' - \log t$	0.377	0.370	0.352
$\log h\gamma'' - \log t$	0.319	0.317	0.337
$\log d\gamma' - \log t$	0.356	0.322	0.295



7 Arrhenius plots for determination of activation energy for growth of  $\gamma''$ - and  $\gamma'$ -phases

where  $N_v$  is the total number of particles/unit volume,  $\rho^2 h(\rho)$  is the theoretical distribution function based on LSW theory, and  $\rho = d/\bar{d}$ .

The number of particles  $N_{v_i}$  in each size class interval  $\Delta$  is defined<sup>2</sup> as

$$N_{v_i} = f(r, t) dr \quad (6)$$

For oblate particles  $dr$  in equation (6) has to be expressed in terms of their aspect ratio ( $q = d/h$ ) to evaluate the distribution function  $\rho^2 h(\rho)$  in equation (5). One can assume that an oblate-ellipsoidal particle becomes almost equal to a disc-shaped particle when  $q$  is very small. Therefore, one can rewrite equation (6) as<sup>16</sup>

$$N_{v_i} = f(d, t) \frac{(2+q)\Delta}{6} \quad (7)$$

Therefore, by combining equations (5) and (7) the distribution function for  $\gamma''$ -particles is given by

$$\rho^2 h(\rho) = \frac{27}{4} \frac{d}{(2+q)\Delta} \frac{N_{v_i}}{N_v} \quad (8)$$

Similarly, the  $\gamma'$ -particles, the distribution function is given by

$$\rho^2 h(\rho) = \frac{9}{4} \frac{\bar{d}}{\Delta} \frac{N_{v_i}}{N_v} \quad (9)$$

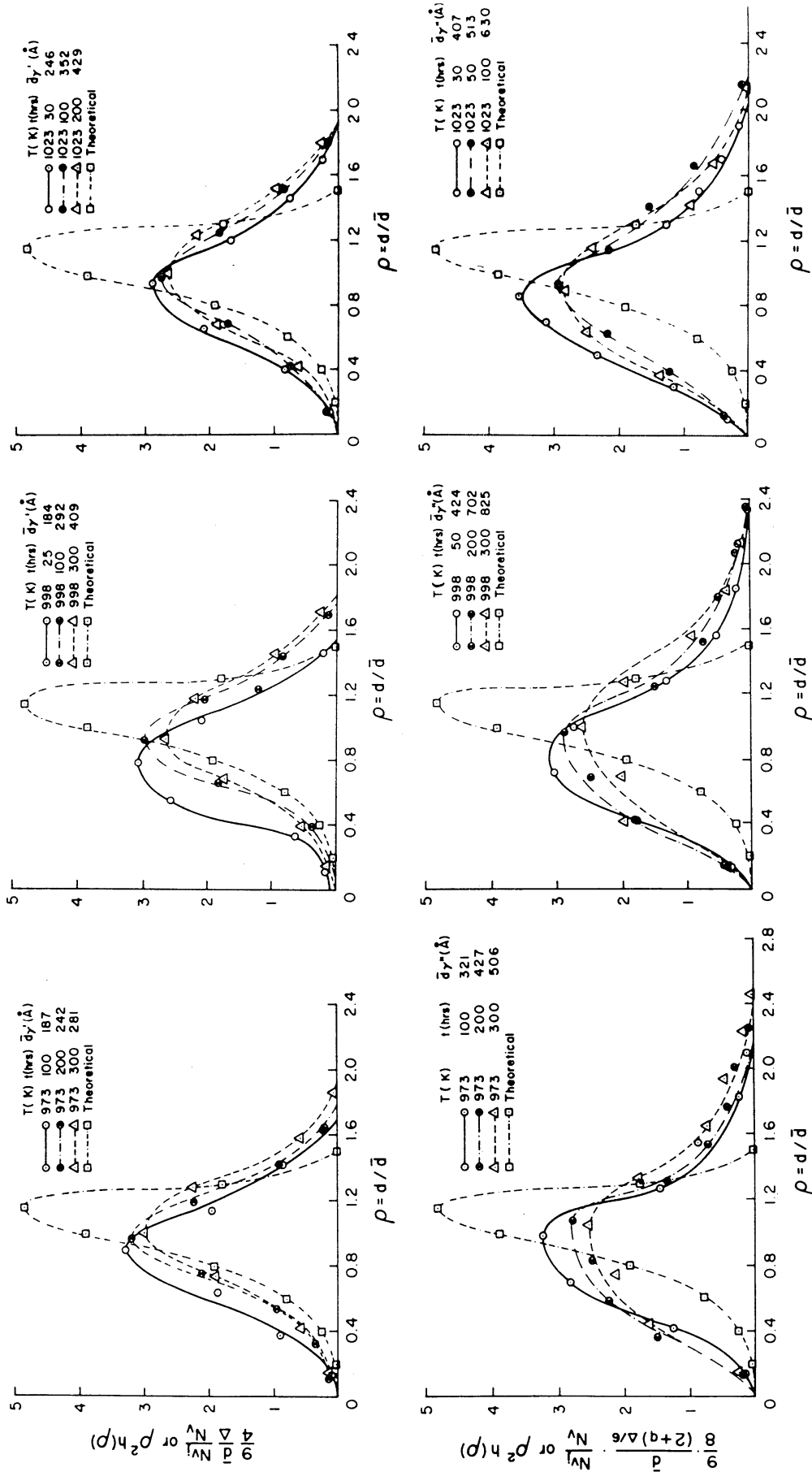
The normalized distribution of  $\gamma''$ - and  $\gamma'$ -particles, plotted against  $\rho$ , after various aging treatments is shown in Fig. 8. This figure also shows the theoretical distribution for comparison with the experimental distribution. It is seen that, compared with the theoretical, the experimental distribution for both  $\gamma''$ - and  $\gamma'$ -particles is much broader and the maxima are also smaller and occur at lower values of  $\rho$ .

#### DISCUSSION

The above results show that one of the basic requirements of the LSW theory of diffusion-controlled growth, i.e. that the

Table 3 Data for determination of activation energy  $Q$

Temperature (T), K	$1/T \times 10^4$	$\gamma''$		$\gamma'$	
		$K'', \text{\AA}^3 \text{s}^{-1}$	$\ln TK''/q$	$K', \text{\AA}^3 \text{s}^{-1}$	$\ln TK'$
973	10.28	$1.26 \times 10^2$	7.270	$0.213 \times 10^2$	5.332
998	10.02	$5.28 \times 10^2$	8.425	$0.627 \times 10^2$	6.438
1023	9.775	$6.94 \times 10^2$	9.074	$1.043 \times 10^2$	6.973



8 Observed and theoretical distribution of  $\gamma''$ - and  $\gamma'$ -particle size after various aging treatments

precipitate size should be proportional to the cube root of the aging time, is satisfied by both the  $\gamma'$  and  $\gamma''$  in Inconel 718 at all three aging temperatures. The activation energy for the growth of  $\gamma''$ - and  $\gamma'$ -phases is nearly the same, i.e. 298 and 271 KJ mol<sup>-1</sup>, respectively. The  $\gamma''$ -phase is based on Ni<sub>3</sub>Nb, and  $\gamma'$  is based on Ni<sub>3</sub>(AlTi); however, extensive amounts of other alloying elements such as Mo, Cr, Fe, etc. will also be present as has been observed in  $\gamma'$ -phase in other alloys.<sup>17,18</sup> That is to say that growth of both of these phases will require diffusion of similar types of elements. Therefore, the activation energy for the growth of  $\gamma''$  as well as  $\gamma'$  should be nearly the same and dependent upon the activation energy for diffusion of Nb, Ti, Al, Fe, Cr, and Mo atoms in Ni. The activation energy for diffusion of Ti and Al in Ni is found to be 257 and 270 KJ mol<sup>-1</sup>, respectively,<sup>19</sup> and that of Fe in the temperature range 923–1223 K in Ni to be 276 KJ mol<sup>-1</sup>.<sup>20</sup> The activation energy for diffusion of Nb in an Ni–Fe–Nb system<sup>21</sup> and Cr in an Ni–Cr system<sup>22</sup> has been reported to be 264 and 250–260 KJ mol<sup>-1</sup> respectively. Therefore, it is seen that the activation energy for the growth of  $\gamma'$ - and  $\gamma''$ -phases is nearly similar to that of diffusion of the solute atoms in Ni and Ni-base alloys. This would also suggest that the growth of  $\gamma'$  and  $\gamma''$  follows the LSW theory of diffusion-controlled growth.

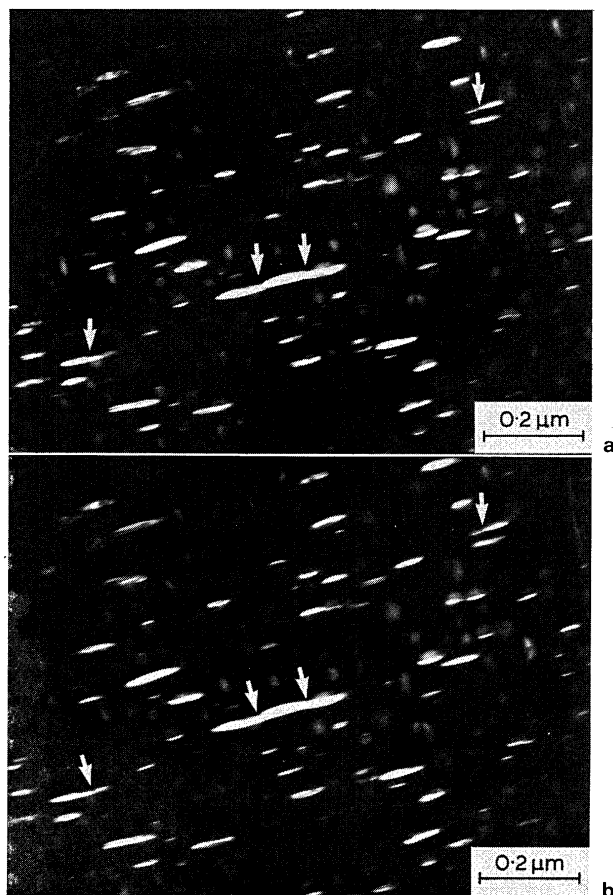
A major discrepancy between the results of the present investigation and the predictions of the LSW theory, however, is observed in the distribution of both the  $\gamma'$ - and  $\gamma''$ -phase particles at all three aging temperatures. According to the LSW theory during the steady-state coarsening process: the distribution of precipitate particles is skewed towards larger particle size, i.e. the maximum occurs at  $\rho = 1.135\bar{d}$  as shown in Fig. 8, and has a sharp cut-off at  $\rho = 1.5\bar{d}$ . The experimental size distributions of both  $\gamma'$  and  $\gamma''$  seem to be in a quasisteady state but they are much broader than the theoretical distribution, especially for  $\gamma''$ -particles, i.e. the maximum cut-off size for  $\gamma'$  is about 1.8 to 2.0 $\bar{d}$  and that for  $\gamma''$  is about 2.2 $\bar{d}$ . The maxima in the distribution curves also occur at smaller values of  $\rho$ , i.e. the degree of skewness is less than the theoretical curve. It is also seen that the peak height of all the distribution curves is a great deal smaller than the theoretically predicted value. The distribution of both the phases, however, is similar to that observed in other  $\gamma'$ - and  $\gamma''$ -precipitation-strengthened alloys. Such a broad distribution has been generally attributed to the presence of lattice misfit between the precipitate and the matrix; the larger the misfit, the larger is the deviation from the theoretical cut-off value of 1.5 $\bar{d}$ .<sup>6</sup> It has been suggested that a large lattice misfit provides a larger strain energy around the particles which increases the driving force for the coalescence of particles resulting in a large cut-off size.<sup>6</sup> This might explain the larger cut-off for  $\gamma''$  than for  $\gamma'$  since the misfit for  $\gamma''$  is 2.86% whereas that for  $\gamma'$  is 0.4%.

Recently, Davies *et al.*<sup>23</sup> have explained the generally observed wider distribution of precipitate particles by the 'encounter' mechanism. The LSW theory is strictly applicable only when the volume fraction of the particles undergoing the coarsening process is nearly zero. All the systems that have been studied so far violate this condition. Davies *et al.*<sup>23</sup> have modified the LSW theory to incorporate the influence of volume fraction on the coarsening process, i.e. by taking into account the effect of encounter, and called it the Lifshitz–Slyozov encounter modified (LSEM) theory.

According to the LSEM theory if, during the coarsening process, a significant amount of second-phase particles is present, the interaction between the diffusion field around

two growing particles may bring their surfaces together causing them to coalesce. When a large particle approaches a small particle, the diffusion field of the larger particle dominates over that of the smaller particle, resulting in a rapid dissolution and coalescence. Such a coalescence of particles increases the growth rate to a small extent and broadens the particle-size distribution, although the rate of change of the mean particle size remains proportional to the cube root of the aging time. The LSEM theory also predicts the particle-size distribution to be more symmetrical and broader compared with that predicted by the LSW theory.

The coalescence of Ni<sub>3</sub>Al particles in an Ni–Co–Al system, in the form of 'necks' and L-shaped particles, has been reported by Davies *et al.*,<sup>23</sup> suggesting the occurrence of the 'encounter' process. In the present investigation, the evidence of 'encounter', in the form of 'necks' between the growing particles, was also observed. Typical examples of 'necks' are marked by arrows in Fig. 9a which is the dark-field structure of a specimen aged for 100 h at 973 K. In this dark-field structure, which is in {100} thin-foil orientation and was taken with a (100) reflection, both  $\gamma''$ - and  $\gamma'$ -particles are visible. To ensure that the 'necks' were the result of 'encounter' or two growing particles approaching each other, and not due to the overlooking of the particles through the thickness of the foil, the same areas were examined over a large degree of tilt angles. For example, after a +10° tilt, the necks observed in Fig. 9a are still seen as 'necks' (and marked by arrows) in Fig. 9b and not as two separate particles being viewed through the thickness of the



a dark-field structure; b dark-field structure after 10° tilt

9 Specimen aged for 100 h at 973 K taken with (100)( $\gamma'' + \gamma'$ ) reflection

foil. It should also be noted that the 'encounter' process may occur not only between two  $\gamma''$ -particles, but also between  $\gamma''$ - and  $\gamma'$ -particles since nearly the same elements constitute both the phases. Therefore, although the volume fraction of  $\gamma'$ -phase is relatively small, i.e. about 3–5%, its growth may also be influenced by 'encounter' by a neighbouring  $\gamma''$ -phase and vice versa. It would seem, therefore, that the distribution curves of  $\gamma'$ - and  $\gamma''$ -particles (which have a larger cut-off value, are nearly symmetrical and have a significantly lower maximum than the theoretical curve) can be explained better by the LSEM theory than the classical LSW theory.

## CONCLUSIONS

1. The disc-shaped ordered bct  $\gamma''$ - and spherical ordered fcc  $\gamma'$ -precipitate particles are present simultaneously in the fcc matrix when Inconel 718 is aged in the 973–1023 K temperature range. The ratio of the volume fraction of  $\gamma''$  and  $\gamma'$  is between 2.5 and 4.0.

2. The coarsening kinetics of both  $\gamma''$ - and  $\gamma'$ -precipitates in this alloy follow the time-law prediction of the Lifshitz–Wagner theory of diffusion-controlled growth.

3. The particle-size distribution of both the phases, however, differs significantly from that predicted by the Lifshitz–Wagner theory. This could be due to the effect of 'encounters' between the growing particles and also due to the presence of large lattice mismatch between the precipitates and the matrix.

## ACKNOWLEDGMENTS

The authors would like to thank the International Nickel Co., Canada, for supplying the alloy and the National Science and Engineering Research Council, Ottawa, for financial support. One of the authors (HY) would also like to thank the Government of the People's Republic of China for financial support.

## REFERENCES

1. M. LIFSHITZ and V. V. SLYOZOV: *J. Phys. Chem. Solids*, 1961, **19**, 35.
2. C. WAGNER: *Z. Electrochem.*, 1961, **65**, 581.
3. A. J. ARDELL and R. B. NICHOLSON: *Acta Metall.*, 1966, **14**, 1295.
4. A. J. ARDELL and R. B. NICHOLSON: *J. Phys. Chem. Solids*, 1966, **27**, 1793.
5. P. K. RASTOGI and A. J. ARDELL: *Acta Metall.*, 1971, **19**, 321.
6. A. J. ARDELL: *Metall. Trans.*, 1970, **1**, 525.
7. M. C. CHATURVEDI and D. W. CHUNG: *J. Inst. Met.*, 1973, **101**, 253.
8. M. C. CHATURVEDI and D. W. CHUNG: *Metall. Trans.*, 1979, **10A**, 1579.
9. M. RAGHAVAN: *Metall. Trans.*, 1977, **8A**, 1071.
10. H. A. MOREEN, R. TAGGART, and D. H. POLONIS: *Metall. Trans.*, 1974, **5**, 79.
11. P. S. KOTVAL: NASA Contract Rep. Cr-52644, Dec. 1969, (quoted in Ref. 10).
12. S. E. AXTER and D. H. POLONIS: *Mater. Sci. Eng.*, 1978, **36**, 71.
13. D. F. PAULONIS, J. M. OBLAK, and D. S. DUVALL: *Trans. ASM*, 1969, **62**, 611.
14. J. W. CAHN and J. NUTTING: *Trans. Metall. Soc. AIME*, 1959, **215**, 526.
15. J. D. BOYD and R. B. NICHOLSON: *Acta Metall.*, 1971, **19**, 1379.
16. P. DEB and M. C. CHATURVEDI: *Metallography*, to be published.
17. J. MIHALISIN and D. PASQUINE: paper presented at Int. Symp. on 'Structural stability in super alloys', Seven Springs, Pa., USA, 1968.
18. O. H. KRIEGE and C. P. SULLIVAN: *Trans. ASM*, 1968, **61**, 278.
19. R. A. SWALIN and A. MARTIN: *Trans. Metall. Soc. AIME*, 1956, **206**, 567.
20. *Diffusion Data J.*: 1973, **7**, 198.
21. *Diffusion Data J.*: 1978, **17**, 62.
22. *Diffusion Data J.*: 1972, **6**, 358.
23. C. K. L. DAVIES, P. NASH, and R. N. STEVENS: *Acta Metall.*, 1980, **28**, 179.

# QUANTITATIVE MICROANALYSIS WITH HIGH SPATIAL RESOLUTION

*Send for your free copy of the 32-page  
Metals Society Publications List*

Proceedings of the conference held in Manchester on 25-27 March 1981 by The Metals Society and The Institute of Physics in view of rapid developments realized during the last five years in the techniques and application of high-resolution

microanalysis, particularly X-ray microanalysis and electron energy loss spectrometry (EELS) of thin specimens. The volume contains 41 papers by authors from the USA and Europe as well as

the UK; discussions; a preface and an introduction; a list of participants; indexes. The four subject areas are: the theory and applications of energy-dispersive X-ray analysis; EELS; instrumentation; convergent beam electron diffraction and other techniques.

Metals Society Book 277 (ISBN 0 904357 38 4)

published in October 1981 x + 278 pages A4 (30 x 21 cm) with over 300 illustrations casebound with jacket

Prices (post-free): to UK address £35.00 (Members £28.00);

to Europe and overseas US\$90.00 (Members \$72.00)

Please order, sending correct remittance and quoting book

no. 277, from Book Sales Department, The Metals Society,

1 Carlton House Terrace, London SW1Y 5DB [01-839 4071]

Book 277

